A Protein Engineering Approach Differentiates the Functional Importance of Carbohydrate Moieties of Interleukin-5 Receptor α

13 AUTHORS, INCLUDING:

Monika M. Jost
Drexel University College of Medicine
29 PUBLICATIONS   1,237 CITATIONS

SEE PROFILE

Gianfranco Pasut
University of Padova
75 PUBLICATIONS   3,195 CITATIONS

SEE PROFILE

Sam Lievens
Ghent University
53 PUBLICATIONS   782 CITATIONS

SEE PROFILE

Irwin Chaiken
Drexel University College of Medicine
66 PUBLICATIONS   1,904 CITATIONS

SEE PROFILE

A Protein Engineering Approach Differentiates the Functional Importance of Carbohydrate Moieties of Interleukin-5 Receptor α

Tetsuya Ishino,[†,⊥] Nicoleta J. Economou,[†] Karyn McFadden,[†] Meirav Zaks-Zilberman,[†] Monika Jost,[‡] Sabine Baxter,[†] Mark R. Contarino,[†] Adrian E. Harrington,[†] Patrick J. Loll,[†] Gianfranco Pasut,[§] Sam Lievens,[∥] Jan Tavernier,[∥] and Irwin Chaiken*[,†]

[†]Department of Biochemistry and Molecular Biology, Drexel University College of Medicine, 11102 New College Building, 245 North 15th Street, Philadelphia, Pennsylvania 19102, United States

[‡]Department of Radiation Oncology, Drexel University College of Medicine, 11102 New College Building, 245 North 15th Street, Philadelphia, Pennsylvania 19102, United States

[§]Department of Pharmaceutical Sciences, University of Padua, Via F. Marzolo 5, Padua 35131, Italy

[∥]Department of Medical Protein Research, Flanders Interuniversity Institute for Biotechnology, VIB09-Faculty of Medicine and Health Sciences, Ghent University, Ghent, Belgium

Ⓢ *Supporting Information*

ABSTRACT: Human interleukin-5 receptor α (IL5Rα) is a glycoprotein that contains four N-glycosylation sites in the extracellular region. Previously, we found that enzymatic deglycosylation of IL5Rα resulted in complete loss of IL5 binding. To localize the functionally important carbohydrate moieties, we employed site-directed mutagenesis at the N-glycosylation sites (Asn[15], Asn[111], Asn[196], and Asn[224]). Because Asn-to-Gln mutagenesis caused a significant loss of structural integrity, we used diverse mutations to identify stability-preserving changes. We also rationally designed mutations at and around the N-glycosylation sites based on sequence alignment with mouse IL5Rα and other cytokine receptors. These approaches were most successful at Asn[15], Asn[111], and Asn[224]. In contrast, any replacement at Asn[196] severely reduced stability, with the N196T mutant having a reduced binding affinity for IL5 and diminished biological activity because of the lack of cell surface expression. Lectin inhibition analysis suggested that the carbohydrate at Asn[196] is unlikely involved in direct ligand binding. Taking this into account, we constructed a stable variant, with triple mutational deglycosylation (N15D, I109V/V110T/N111D, and L223R/N224Q). The re-engineered protein retained Asn[196] while the other three glycosylation sites were eliminated. This mostly deglycosylated variant had the same ligand binding affinity and biological activity as fully glycosylated IL5Rα, thus demonstrating a unique role for Asn[196] glycosylation in IL5Rα function. The results suggest that unique carbohydrate groups in multiglycosylated receptors can be utilized asymmetrically for function.
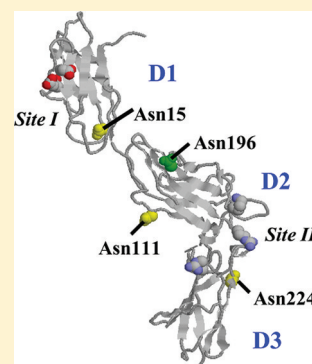
Interleukin-5 (IL5) is a hematopoietic growth factor that promotes maturation, proliferation, and activation of eosinophils.[1] Although eosinophils play a major role in host defense by combating parasites, they are also central to tissue damage in several allergic disorders, including asthma and hypereosinophilic syndrome.[2−4] Hence, IL5 has been implicated in the pathogenesis of these inflammatory diseases.

IL5 exerts its effects through its cognate receptor on the cell surface of eosinophils. The IL5 receptor is composed of an α subunit that binds IL5 specifically and a βc subunit that shares affinity for IL3 and GM-CSF and is responsible for cytoplasmic signal transduction. Data from cell FRET and other biochemical analyses suggest an activation model in which IL5 triggers cellular responses by sequentially binding first to IL5Rα followed by binding of the complex to a preassembled βc subunit.[5−8]

We and others have investigated the structural elements underpinning molecular recognition in the complex between IL5 and IL5Rα and have identified important characteristics of epitope usage. The receptor binding elements in IL5 are dominated by charged residues in helix B (His[38], Lys[39], and His[41]), the C−D turn (Glu[88], Glu[89], Arg[90], and Arg[91]), and helix D (Glu[110]).[9,10] For βc binding and signal transduction, Glu[13] in helix A is a key residue.[10] The ligand binding residues in IL5Rα also are charged. These are located in domain 1 (Asp[55], Asp[56], and Glu[58]), domain 2 (Lys[186] and Arg[188]), and domain 3 (Arg[297]) of the three fibronectin-type III domains of the extracellular region of IL5Rα.[11,12] A homology model of the IL5−IL5Rα complex provided supporting evidence that a pair of complementary charged interfaces plays an important role in the specific interaction between IL5 and IL5Rα.[12] Moreover, thermodynamic studies suggest that IL5Rα is likely to undergo significant conformational rearrangement upon ligand binding, which might be important for βc recruitment and subsequent

receptor activation.[13] Such complementary charge–charge interactions and ensuing conformational rearrangement are likely the key steps in receptor activation.

While the biological function of a protein is primarily determined by its polypeptide sequence, glycosylation can have an impact on many aspects of its activity, such as intracellular trafficking, membrane secretion, folding, structure, stability, solubility, and interactions with binding partners.[14−16] IL5Rα is a glycoprotein that contains four N-glycosylation sites (Asn[15], Asn[111], Asn[196], and Asn[224]) in the extracellular region, and it was shown that ~14% of the total mass of the extracellular region of IL5Rα is carbohydrate.[13] Previously, it was found that IL5Rα deglycosylated by PNGase F could not bind to IL5, suggesting the importance of receptor glycosylation for stabilizing the structure of the receptor itself and/or receptor–ligand interaction.[13] However, it has remained unclear how glycosylation affects the ligand binding activity of IL5Rα and whether individual glycosylation sites play a more important role than others. In this study, we investigated the functional roles of each of the four glycosylation sites in ligand binding activity, biological function, and cell surface expression of IL5Rα. Because our initial trial of Asn-to-Gln mutagenesis caused a significant loss of stability judging from its binding to a conformationally sensitive antibody, we employed a more sophisticated protein engineering approach by combining apolar-to-polar mutations and homology-based mutagenesis.[17,18] This work led to a stable variant in which three of four glycosylation sites are eliminated (N15D, I109V/V110T/N111D, and L223R/N224Q). This mostly deglycosylated variant retained the same ligand binding affinity and biological activity as fully glycosylated IL5Rα. We demonstrated in this work that protein engineering is a useful tool for identifying functionally critical glycosylation sites and deriving tools for structural analysis of other glycoproteins.

■ EXPERIMENTAL PROCEDURES

Materials. Concanavalin A (ConA), bovine serum albumin (BSA), and mouse interleukin-3 (IL3) were purchased from Sigma-Aldrich (St. Louis, MO). Human interleukin-5 (IL5) and cyanovirin-N (CV−N) were produced and purified as previously described.[19,20] All the enzymes were purchased from New England Biolabs (Beverly, MA). All oligo DNA primers, *Drosophila* Schneider 2 (S2) cells, cell culture medium, L-glutamine solution, and RPMI 1640 medium were purchased from Invitrogen (Carlsbad, CA). The BaF3 cell line was purchased from German Collection of Microorganisms and Cell Cultures (DSMZ, Braunschweig, Germany). For surface plasmon resonance measurements (SPR), sensor chip CM5, surfactant P20, N-ethyl-N-[3-(dimethylamino)propyl]-carbodiimide (EDC), N-hydroxysuccinimide (NHS), 1 M ethanolamine (pH 8.5), and 10 mM glycine hydrochloride (glycine-HCl) (pH 1.5 and 2.0) were purchased from Biacore (Piscataway, NJ).

S2 Cell Transient Expression of Soluble IL5Rα. For mutational deglycosylation of soluble IL5Rα, site-directed mutagenesis was introduced into pMT-IL5Rα-V5-His[12] using a QuikChange site-directed mutagenesis kit (Stratagene). The presence of the desired mutations was verified by DNA sequencing. *Drosophila* S2 cells were transiently transfected with vector pMT-IL5Rα-V5-His together with pMT-GFP [expression vector for green fluorescent protein (Invitrogen)] using Cellfectin reagent (Invitrogen) and grown in serum-free

medium supplemented with 20 mM L-glutamine. Protein expression was induced by addition of 650 μM copper sulfate 3 days after transfection. Cell-free supernatant was collected after 2 days and stored at −20 °C for the following binding analysis.

Protein Purification. *Soluble IL5Rα.* The soluble forms of human IL5Rα and its deglycosylated variant with N15D, I109V/V110T/N111D, and L223R/N224Q mutations (denoted IL5Rα[ΔN15/111/224]) were produced in stably transfected *Drosophila* S2 cells. The *Drosophila* expression vector and blasticidin-resistant vector pCoBlast (Invitrogen) were cotransfected into S2 cells using Cellfectin reagent (Invitrogen). Blasticidin-resistant cells were selected as a stable polyclonal population and grown in serum-free medium supplemented with 20 mM L-glutamine and 25 μg/mL blasticidin S (Invitrogen). For expression, the cell density was expanded to approximately 1 × 10^7 cells/mL and protein expression was induced by addition of 0.6 mM copper sulfate. The culture was harvested after 72 h and centrifuged at 1000g for 10 min. The soluble forms of IL5Rα and the deglycosylated variant were purified as described previously.[7] Briefly, the cleared supernatant was loaded onto a 2B6R-conjugated affinity column, and bound proteins were eluted with 0.1 M glycine (pH 2.8). The resulting protein solution was neutralized with a 1 M Tris-HCl solution (pH 9.0), buffer exchanged to PBS, concentrated, and stored below −80 °C. The ligand binding activity was confirmed by an SPR binding assay as described previously.[12]

Anti-IL5Rα Monoclonal Antibody. 2B6R and α16 are mouse monoclonal antibodies raised against soluble IL5Rα.[7,21] The hybridoma cells were maintained in RPMI 1640 medium with 10% FCS (Hyclone). Antibodies were purified by using protein G affinity column chromatography according to a standard procedure.

Protein Characterization. The purity of the protein was confirmed by Western blot analyses using polyacrylamide gel electrophoresis in the presence of 0.1% sodium dodecyl sulfate (SDS−PAGE). The integrity of proteins was verified by matrix-assisted laser desorption ionization mass spectrometry (MALDI-MS) (Wistar Institute, Philadelphia, PA). Protein quantitation was achieved by measuring the absorbance at 280 nm and calculating the concentration using the molar absorption coefficient using the method of Pace et al.[22]

SPR Biosensor Binding Analysis. The kinetic interaction assay was conducted using an SPR biosensor, Biacore 3000 (Biacore Inc., Uppsala, Sweden). All the experiments were conducted at 25 °C in PBS buffer containing 0.005% P20.

Screening Assay for the Structural Integrity of IL5Rα Deglycosylation Mutants. We used four different antibodies, namely, 17b (anti-HIV gp120 mAb[23]), anti-GFP pAb (Clontech), anti-V5-tag pAb (Invitrogen), and α16 (anti-human IL5Rα mAb[21]). For immobilization of the antibodies on a CM5 sensor chip, a 1 mg/mL protein stock solution was diluted 50-fold in 10 mM acetate (pH 4.5) and injected onto a biosensor surface that had been preactivated with a 1:1 mixture of 200 mM EDC and 50 mM NHS, followed by the injection of 1 M ethanolamine hydrochloride (pH 8.5). Transiently expressed IL5Rα mutational variants were injected over the antibody-immobilized surface. After the surface had been washed, the amount of bound protein was measured for each antibody surface. To regenerate chip surfaces, bound proteins
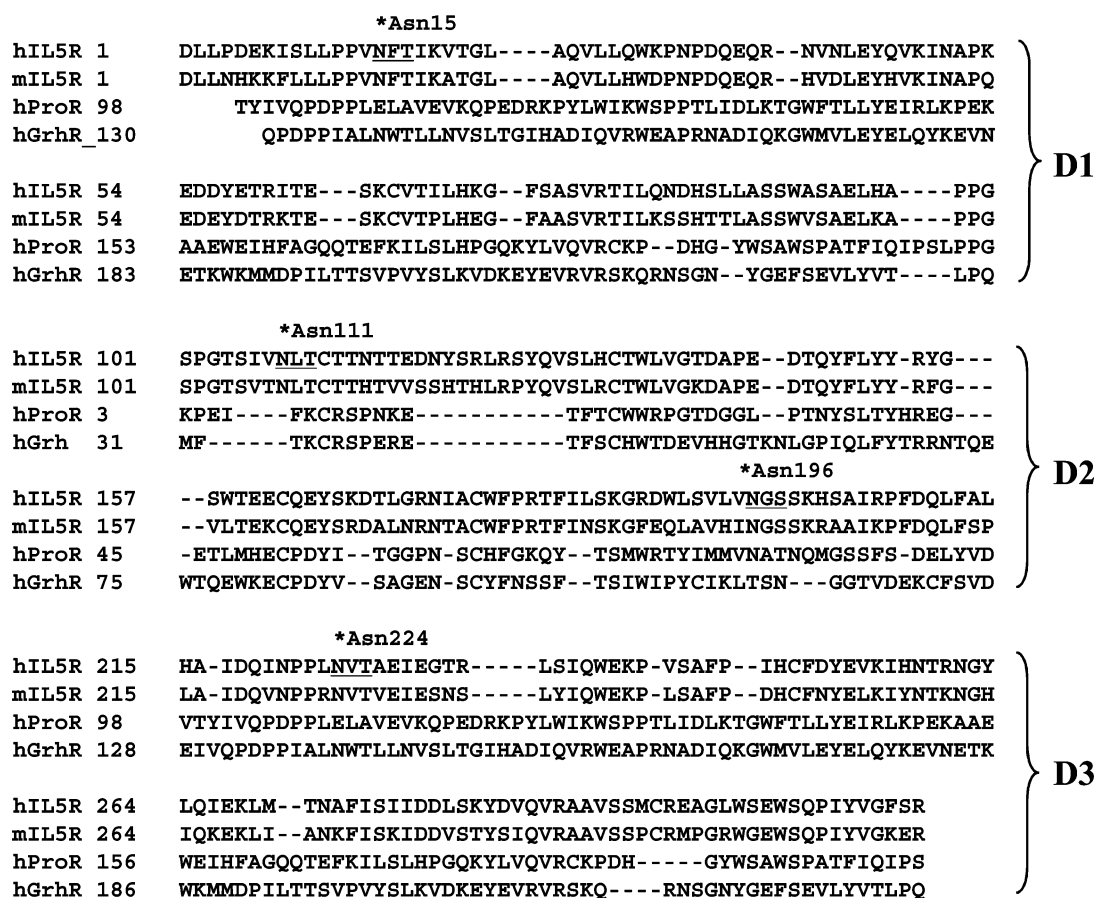
```
                          *Asn15
        hIL5R   1    DLLPDEKISLLPPVNFTIKVTGL----AQVLLQWKPNPDQEQR--NVNLEYQVKINAPK  ⎫
        mIL5R   1    DLLNHKKFLLLPPVNFTIKATGL----AQVLLHWDPNPDQEQR--HVDLEYHVKINAPQ  ⎪
        hProR  98       TYIVQPDPPLELAVEVKQPEDRKPYLWIKWSPPTLIDLKTGWFTLLYEIRLKPEK     ⎬
        hGrhR_130           QPDPPIALNWTLLNVSLTGIHADIQVRWEAPRNADIQKGWMVLEYELQYKEVN     ⎪
                                                                                     ⎪
                                                                                     ⎬ D1
        hIL5R  54    EDDYETRITE---SKCVTILHKG--FSASVRTILQNDHSLLASSWASAELHA----PPG  ⎪
        mIL5R  54    EDEYDTRKTE---SKCVTPLHEG--FAASVRTILKSSHTTLASSWVSAELKA----PPG  ⎪
        hProR 153    AAEWEIHFAGQQTEFKILSLHPGQKYLVQVRCKP--DHG-YWSAWSPATFIQIPSLPPG  ⎪
        hGrhR 183    ETKWKMMDPILTTSVPVYSLKVDKEYEVRVRSKQRNSGN--YGEFSEVLYVT----LPQ  ⎭


                          *Asn111
        hIL5R 101    SPGTSIVNLTCTTNTTEDNYSRLRSYQVSLHCTWLVGTDAPE--DTQYFLYY-RYG---  ⎫
        mIL5R 101    SPGTSVTNLTCTTHTVVSSHTHLRPYQVSLRCTWLVGKDAPE--DTQYFLYY-RFG---  ⎪
        hProR   3    KPEI----FKCRSPNKE----------TFTCWWRPGTDGGL--PTNYSLTYHREG---  ⎪
        hGrh   31    MF------TKCRSPERE----------TFSCHWTDEVHHGTKNLGPIQLFYTRRNTQE  ⎪
                                                     *Asn196                         ⎬ D2
        hIL5R 157    --SWTEECQEYSKDTLGRNIACWFPRTFILSKGRDWLSVLVNGSSKHSAIRPFDQLFAL  ⎪
        mIL5R 157    --VLTEKCQEYSRDALNRNTACWFPRTFINSKGFEQLAVHINGSSKRAAIKPFDQLFSP  ⎪
        hProR  45    -ETLMHECPDYI--TGGPN-SCHFGKQY--TSMWRTYIMMVNATNQMGSSFS-DELYVD  ⎪
        hGrhR  75    WTQEWKECPDYV--SAGEN-SCYFNSSF--TSIWIPYCIKLTSN---GGTVDEKCFSVD  ⎭


                          *Asn224
        hIL5R 215    HA-IDQINPPLNVTAEIEGTR-----LSIQWEKP-VSAFP--IHCFDYEVKIHNTRNGY  ⎫
        mIL5R 215    LA-IDQVNPPRNVTVEIESNS-----LYIQWEKP-LSAFP--DHCFNYELKIYNTKNGH  ⎪
        hProR  98    VTYIVQPDPPLELAVEVKQPEDRKPYLWIKWSPPTLIDLKTGWFTLLYEIRLKPEKAAE  ⎪
        hGrhR 128    EIVQPDPPIALNWTLLNVSLTGIHADIQVRWEAPRNADIQKGWMVLEYELQYKEVNETK  ⎪
                                                                                     ⎬ D3
        hIL5R 264    LQIEKLM--TNAFISIIDDLSKYDVQVRAAVSSMCREAGLWSEWSQPIYVGFSR       ⎪
        mIL5R 264    IQKEKLI--ANKFISKIDDVSTYSIQVRAAVSSPCRMPGRWGEWSQPIYVGKER       ⎪
        hProR 156    WEIHFAGQQTEFKILSLHPGQKYLVQVRCKPDH-----GYWSAWSPATFIQIPS       ⎪
        hGrhR 186    WKMMDPILTTSVPVYSLKVDKEYEVRVRSKQ----RNSGNYGEFSEVLYVTLPQ       ⎭
```

Figure 1. Sequence alignment of the extracellular domain of IL5Rα and other cytokine receptors. Multiple-sequence alignments of human and mouse IL5Rα, human prolactin receptor, and human growth hormone receptor were performed by using ClustalW version 1.60[49] and further adjusted manually. Three fibronectin type III domains of IL5Rα are denoted D1, D2, and D3.

were removed from the antibody surfaces with 10 mM glycine-HCl (pH 1.6).

Interaction between IL5 and IL5Rα Deglycosylation Mutants. To determine the binding affinity for IL5, we employed a previously established "on-chip purification" method,[12] in which culture medium containing the V5-tagged receptor protein was injected over an anti-V5 antibody surface. Analogous to affinity column chromatography, only the tagged receptor was precaptured on the chip surface, while all of the nonspecific components were washed away. Subsequently, various concentrations of IL5 were injected into the flow cell containing a particular precaptured IL5Rα deglycosylated variant as well as a control surface. To regenerate the chip surfaces, both captured and bound proteins were removed from the antibody surfaces by double injections of a 10 mM glycine-HCl solution (pH 1.6). For this sensor assay, all procedures were automated to create repetitive cycles of injection of cell-free culture (10 μL/min), 0–40 nM IL5 (50 μL/min), and regeneration buffer (100 μL/min). The injection time for the variants was varied to achieve a similar extent of capturing (approximately 200 RU). For the IL5Rα[ΔN196] variant, the binding assay was conducted with a higher-density receptor surface (up to 800 RU).

Lectin Binding and Inhibition Assay. Immobilization of lectins (ConA and CV-N) on a CM5 sensor chip was conducted by the amine coupling method as described above. The real-time interaction was measured by injecting purified IL5Rα or IL5Rα[ΔN15/111/224] onto these surfaces. Bound proteins were removed from the surfaces by triple injections of 10 mM glycine-HCl (pH 1.6) after each cycle. All the procedures were automated to create repetitive cycles of injection of various concentrations of purified IL5Rα or IL5Rα[ΔN15/111/224] (flow rate of 50 μL/min), and regeneration buffer (flow rate of 100 μL/min). To examine whether CV-N affects the IL5–IL5Rα[ΔN15/111/224] interaction, different concentrations of IL5 were passed over the IL5Rα[ΔN15/111/224] captured by CV-N or α16 (control).

Data Analysis. Nonlinear least-squares analysis was used to calculate the association and dissociation rate constants (k_{on} and k_{off}, respectively). Prior to the calculation, the binding data were corrected for nonspecific interaction by subtracting the reference surface data from the reaction surface data and further corrected for the buffer effect by subtracting the signal due to buffer injections from those of protein sample injections.[24] The interaction curves thus obtained were globally fit using a model for 1:1 Langmuir binding (BIAevaluation, Biacore). Individual kinetic parameters were obtained from at least three separate experiments. The equilibrium dissociation constant (K_d) was calculated with the relationship $K_d = k_{off}/k_{on}$.

Construction of BaF3 Cell Lines Expressing Full-Length IL5Rα. Mammalian expression vector pcDNA3.1 (Invitrogen) encoding full-length IL5Rα was subcloned by using pSV-SPORT-IL5Rα[25] as a template. For full-length IL5Rα[ΔN196] and full-length IL5Rα[ΔN15/111/224], mutations were introduced into the pcDNA for full-length IL5Rα

using QuikChange site-directed mutagenesis kit (Stratagene). The mouse pro B lymphocyte IL3-dependent cell line, BaF3, was maintained in RPMI 1640 medium with 10% FCS (Hyclone) supplemented with 10 nM mouse IL3. For transfection, cells (2×10^6) were washed with PBS buffer and then incubated in 0.8 mL of PBS buffer containing 50 μg of DNA for 10 min at 4 °C. Electroporation was performed using Gene Pulser II (Bio-Rad) at 300 V and 975 μF. Subsequently, the cells were allowed to recover from transfection in the IL3-supplemented growth medium. Selection was initiated 48 h after transfection in the IL3-supplemented growth medium containing 600 μg/mL G418 (Invitrogen). After 8−10 days, healthy populations of cells were obtained and maintained.

Cell Proliferation Assay. The assay was conducted using BaF3 cells expressing full-length IL5Rα. These cells were washed four times in RPMI 1640 medium with 10% FCS (Hyclone) to remove residual mouse IL3 from the culture medium. Plates with 96 wells were seeded with 5000 cells/well (50 μL) and incubated for 48 h (37 °C and 5% CO_2) in the presence of different concentrations of human IL5 (50 μL). Following the 48 h incubation, 10 μL of WST-1 {4-[3-(4-iodophenyl)-2-(4-nitrophenyl)]-2H-5-tetrazolio-1,3-benzene disulfonate (Roche Diagnostics)} was added to each well and incubated for 4 h (37 °C). The plate was then read using a microplate reader at an absorbance of 450 nm with a 650 nm reference. Individual values were obtained from three experiments, and the average values with the standard deviation were plotted using Excel (Microsoft). To obtain the ED_{50} value, the average values were fitted to a sigmoidal dose−response model using Prism (GraphPad).

Flow Cytometry. For staining, cells were suspended in staining buffer (PBS with 10% BSA) and incubated with 20 μg/mL α16 or 2B6R as the primary antibody or 17b as an isotype-matched control, for 30 min at 4 °C, followed by incubation with 20 μg/mL Alexa Fluor 488-conjugated goat anti-mouse secondary antibody (Invitrogen) for 45 min at 4 °C. Cells were washed with staining buffer between antibody incubations. Flow cytometry analysis was performed using a FACSORT flow cytometer (BD Biosciences, San Diego, CA) with 488 nm excitation from an argon ion laser at 15 mW. The forward scatter threshold was set to exclude small debris. Alexa Fluor 488 log fluorescence was captured on the FL1 channel equipped with a 530 nm wavelength filter with a 30 nm bandwidth. Data were acquired using Lysis II (version 2.0, BD Biosciences). At least 10000 events were acquired per sample. Data analysis was performed using WinMDI (version 2.8, J. Trotter, Scripps Research Institute, La Jolla, CA, available at http://www.facs.scripps.edu).

Homology Modeling. The three-dimensional structure of IL5Rα[ΔN15/111/224] was modeled using MODELLER 6v2.[26] The previously reported modeled structure of wild-type IL5Rα[12] was used as a template. Basic steric principles such as close contacts or violation of stereochemistry were examined using PROCHECK,[27] and the three-dimensional profiles of the models were examined using ProsaII.[28] On the basis of these quality checks, the best modeled structure was chosen.

■ RESULTS

Assessment of the Structural Integrity of IL5Rα. To define the functional roles of each N-linked carbohydrate moiety at Asn[15], Asn[111], Asn[196], and Asn[224] of IL5Rα (Figure

1), we performed site-directed mutagenesis at the N-glycosylation sites and investigated both the ligand binding activity and the structural integrity of the mutants. The extracellular region of IL5Rα was fused with the V5-tag peptide at its C-terminus and was expressed in S2 cells as described previously.[12] Prior to functional analyses of deglycosylation mutants of IL5Rα, we first tested whether the mutations could affect the structural integrity of IL5Rα. We previously found that an anti-IL5Rα mAb α16[21] recognizes a three-dimensional epitope of IL5Rα.[12] In this study, we demonstrated that the soluble form of IL5Rα protein denatured via SDS−PAGE was detected by anti-IL5Rα mAb, 2B6R, and anti-V5-tag antibody while it was not detected by α16 (Figure 2A). These findings suggest that α16 is a conformationally sensitive antibody. We developed a high-throughput assay in which α16 was immobilized on a biosensor surface to examine the stability of transiently expressed proteins. The anti-V5-tag antibody was also immobilized onto a different biosensor chip surface to normalize the expression level of the protein. As a proof of concept, we demonstrated that heat-denatured purified IL5Rα was bound to the anti-V5-tag antibody but failed to bind to α16 (Figure 2B), whereas native IL5Rα was bound to both α16 and the anti-V5-tag antibody (Figure 2C). Thus, we employed this method to verify the structural integrity of various deglycosylated mutants of IL5Rα.

Design of Mutationally Deglycosylated IL5Rα Variants. We first used diverse mutations to identify conformation-preserving changes at Asn[15], Asn[111], Asn[196], and Asn[224], the four glycosylation sites in IL5Rα. For replacement of asparagine, we chose four charged residues (aspartic acid, glutamic acid, lysine, and arginine), one neutral residue (glutamine), and one hydrophobic residue (valine), all of which have molecular volumes similar to that of asparagine. Deglycosylated mutants were transiently expressed and subjected to the structural integrity assay described above. The data are shown in Figure 3. Mutations such as N15D, N111D, and N224K displayed significantly increased stabilities relative to those of Asn-to-Gln mutations (Figure 3A). Of note, replacement with valine at any of the glycosylation sites largely reduced the level of α16 binding, indicating that the four N-glycosylation sites are exposed to the solvent, and thus, the hydrophobic residue introduced at these positions might destabilize the structure of IL5Rα. Because replacement of Asn[196] with any of these six residues severely reduced stability, we expanded mutations of Asn[196] to all other amino acid residues except cysteine, which could cause dimerization of IL5Rα. We found that the Asn-to-Thr mutation was the best among those replacements (Figure 3B).

Second, we designed several mutations on the basis of a hypothesis that apolar-to-polar mutations on the protein surface should increase the stability of the protein. We chose the hydrophobic residues that are exposed to solvent and adjacent to the N-glycosylation sites in the modeled structure of IL5Rα[12] and generated double or triple mutations in those regions based on sequence alignment with mouse IL5Rα, human prolactin receptor, and human growth hormone receptor (Figure 1). The extracellular domains of prolactin and growth hormone receptors were produced in *Escherichia coli*, and their crystal structures in complex with their ligand have been determined,[29,30] indicating the structural stability of the deglycosylated forms. We found that mutants such as I109V/V110T/N111Q, I109V/V110T/N111D, and L223R/
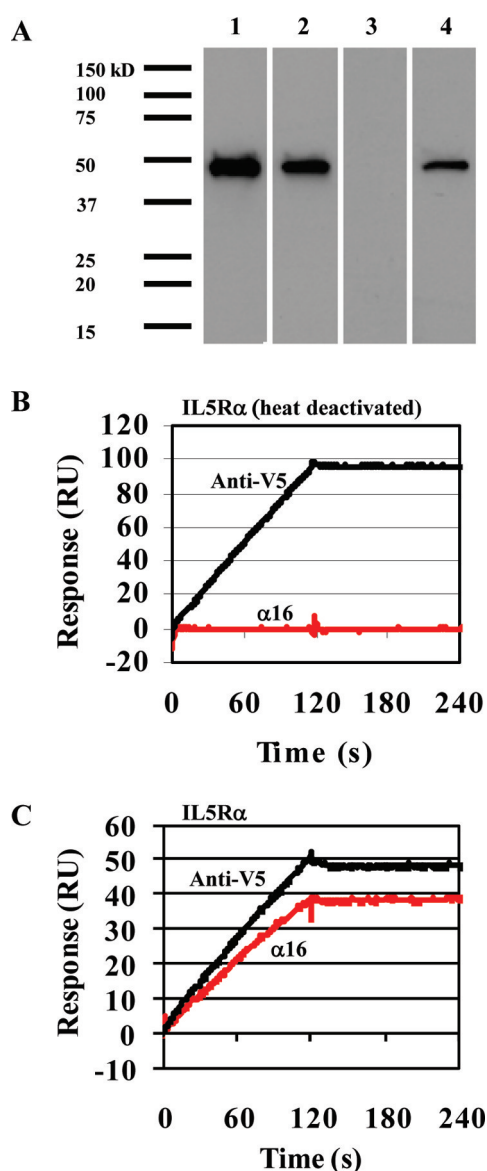
Figure 2. Characterization of a conformationally sensitive anti-IL5Rα antibody. (A) Western blotting of the expressed soluble domain of IL5Rα. The conditioned medium containing soluble IL5Rα was mixed with SDS buffer, boiled for 10 min, and loaded onto an SDS−PAGE gel: lane 1, band stained with anti-IL5Rα mAb (R&D Systems); lane 2, anti-V5-tag pAb (Invitrogen); lane 3, anti-IL5Rα mAb α16; lane 4, anti-IL5Rα mAb 2B6R. (B and C) Injection of the heat-deactivated form of purified IL5Rα (B) or the native form of purified IL5Rα (C) at 0 s, followed by injection of running buffer at 120 s. In this assay, either form of IL5Rα protein was injected over the antibody surfaces, and binding of IL5Rα to each antibody was monitored. Black lines show the sensorgrams for anti-V5-tag pAb and red lines those for α16.

N224Q had almost the same stability as the fully glycosylated form (Figure 3C).

Ligand Binding Activities of Deglycosylated Mutants. For the ligand binding assay, we chose the most stable deglycosylated mutants at each site. These were N15D (denoted IL5Rα[ΔN15]), I109V/V110T/N111D (denoted IL5Rα[ΔN111]), N196T (denoted IL5Rα[ΔN196]), and L223R/N224Q (denoted IL5Rα[ΔN224]). To validate the kinetic interaction with IL5, we employed a previously established SPR biosensor assay.[12] Briefly, different concen-

trations of IL5 were injected over the IL5Rα variants that had been precaptured via their C-terminal V5-tag by the anti-V5-tag antibody immobilized covalently on the biosensor surface (Figure 4). Kinetic analysis showed that deglycosylation variants such as IL5Rα[ΔN15], IL5Rα[ΔN111], and IL5Rα-[ΔN224] had almost the same kinetic profiles as fully glycosylated IL5Rα, whereas IL5Rα[ΔN196] showed a 5-fold increase in its K_d value because of the combination of a decreased k_{on} and an increased k_{off} (Table 1). Our attempt to obtain a completely deglycosylated IL5Rα by using these four mutations resulted in the complete loss of ligand binding and α16 binding (data not shown). Because the N196T mutation is most likely the mutation that destabilized the structure of IL5Rα (Figure 3), we performed triple-mutational deglycosylation with N15D, I109V/V110T/N111D, and L223R/N224Q but maintained Asn[196] glycosylation to obtain the mostly deglycosylated form of IL5Rα. This variant, which had three of four glycosylation sites eliminated (denoted IL5Rα[ΔN15/111/224]), showed the same ligand binding affinity and kinetic parameters as fully glycosylated IL5Rα (Figure 4 and Table 1).

Effect of Lectin on the IL5−IL5Rα Interaction. We conducted further biochemical characterizations of purified IL5Rα[ΔN15/111/224] to elucidate the functional role of the carbohydrate moiety at Asn[196]. MALDI-MS analysis of purified IL5Rα showed that the mass of total carbohydrates was 5873 Da, that is, 14% of the total mass of IL5Rα (Table 2). On the other hand, the mass of total carbohydrates of IL5Rα[ΔN15/111/224] was 2344 Da, that is, 6% of the total mass of IL5Rα[ΔN15/111/224]. These results indicate that a single carbohydrate moiety at Asn[196] occupies as much as 40% of the total carbohydrate content of IL5Rα. To examine the glycosylation at Asn[196], we characterized the lectin binding activity of IL5Rα[ΔN15/111/224] using an SPR biosensor. In this assay, either concanavalin A (ConA) or cyanovirin-N (CV-N) was immobilized on the biosensor surface, and then either purified IL5Rα[ΔN15/111/224] or purified IL5Rα was injected over the lectin surface. We found that the lectin binding affinity of IL5Rα[ΔN15/111/224] was lower than that of fully glycosylated IL5Rα (Figure S1 of the Supporting Information), probably because of the reduced carbohydrate content of IL5Rα[ΔN15/111/224]. Because CV-N selectively binds to high-mannose oligosaccharides, the carbohydrate moiety at Asn[196] might be high-mannose, which is consistent with the previous observations on the carbohydrate structure of IL5Rα.[13]

To test whether the carbohydrate at Asn[196] is involved in the IL5−IL5Rα interaction, we examined binding of IL5 to IL5Rα[ΔN15/111/224] in the presence of CV-N. In this assay, purified IL5Rα[ΔN15/111/224] was captured by CV-N immobilized on the biosensor surface and then nonglycosylated IL5 was injected over the receptor surface. We found that IL5Rα[ΔN15/111/224] binds IL5 with high affinity even when the single carbohydrate group at Asn[196] is occupied by binding to CV-N (Figure S2 of the Supporting Information). This IL5 binding activity suggests that the carbohydrate at Asn[196] of IL5Rα is not involved in a direct contact with IL5.

Biological Activity and Cell Surface Expression. We asked whether N-glycosylation plays a role in the cellular function of IL5Rα. Plasmids encoding the full length of the two deglycosylated variants (IL5Rα[ΔN196] and IL5Rα[ΔN15/111/224]) as well as wild-type IL5Rα were stably transfected into BaF3 cells, and IL5-induced cell proliferation in these cells
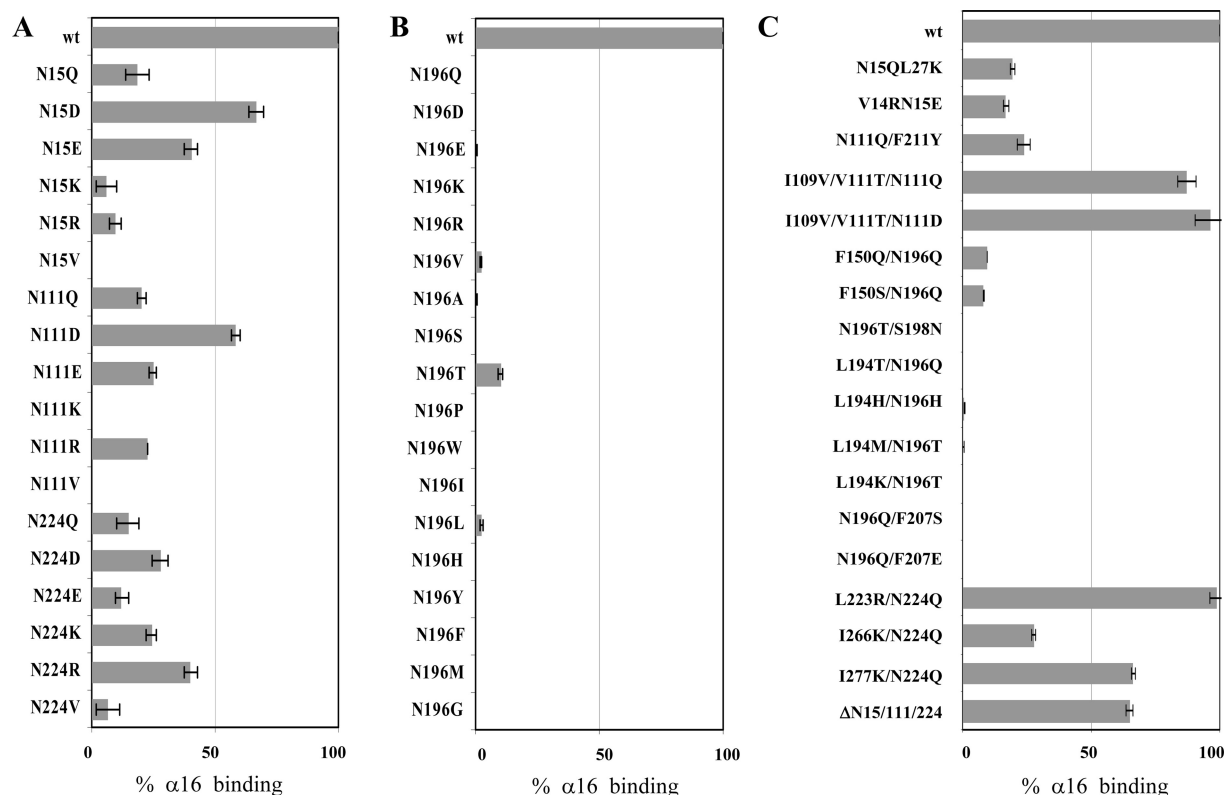
A

wt
N15Q
N15D
N15E
N15K
N15R
N15V
N111Q
N111D
N111E
N111K
N111R
N111V
N224Q
N224D
N224E
N224K
N224R
N224V

0   50   100
% α16 binding

B

wt
N196Q
N196D
N196E
N196K
N196R
N196V
N196A
N196S
N196T
N196P
N196W
N196I
N196L
N196H
N196Y
N196F
N196M
N196G

0   50   100
% α16 binding

C

wt
N15QL27K
V14RN15E
N111Q/F211Y
I109V/V111T/N111Q
I109V/V111T/N111D
F150Q/N196Q
F150S/N196Q
N196T/S198N
L194T/N196Q
L194H/N196H
L194M/N196T
L194K/N196T
N196Q/F207S
N196Q/F207E
L223R/N224Q
I266K/N224Q
I277K/N224Q
ΔN15/111/224

0   50   100
% α16 binding

Figure 3. Screening assay of the structural integrity of soluble forms of deglycosylation mutants. In this assay, culture supernatant containing IL5Rα mutational variants was injected over the immobilized antibody α16 SPR chip surface. This antibody surface was used to examine the stability of transiently expressed proteins, while the anti-V5-tag antibody was used to normalize the expression level of the protein. Thus, the ratio of α16 binding activity to anti-V5 activity denotes the extent of conformational intactness of the expressed proteins. The percent α16 binding level was calculated by dividing amounts of α16-binding proteins by those of anti-V5-tag antibody and then by dividing the resulting values of mutants by that of wild-type IL5Rα. Individual values were obtained from three experiments. The average values are shown as bars, and standard deviations are shown as lines.

was investigated. BaF3 is an IL3-dependent mouse pro B cell line that intrinsically expresses the βc receptor subunit. Because human IL5 and IL5Rα can cross-react with mouse βc, this cell line has been used for the functional analyses of IL5Rα mutational variants.[25] Cells transfected with full-length IL5Rα-[ΔN15/111/224] exhibited IL5-induced cell proliferation similar to that found with fully glycosylated IL5Rα (Figure 5), indicating that N-glycosylations at Asn[15], Asn[111], and Asn[222] of IL5Rα are not important for the cell proliferation activity of the receptor. On the other hand, cells transfected with full-length IL5Rα[ΔN196] exhibited no proliferation (Figure 5A). To determine whether the N196T mutation completely suppressed the biological function because of the absence of the receptor on the cell surface, we assessed the cell surface expression of the deglycosylated mutant with anti-IL5Rα antibodies. Flow cytometry analysis revealed no signal shift in BaF3 cells transfected with full-length IL5Rα[ΔN196], whereas signal shifts were detected in BaF3 cells transfected with either fully glycosylated IL5Rα or IL5Rα[ΔN15/111/224] (Figure 5B). These data indicate that IL5Rα[ΔN196] was not expressed on the cell. Hence, N-glycosylation at Asn[196] might be required for transport of IL5Rα to the cell surface.

■ DISCUSSION

We have previously shown the effects of amino acid replacement of human IL5Rα on ligand binding and receptor antagonism.[12,31,32] The main purpose of this study was to

provide insights into the specific roles of N-glycosylation of IL5Rα in its structure and function. IL5Rα contains four consensus N-glycosylation sites (Asn-X-Ser/Thr) at Asn[15], Asn[111], Asn[196], and Asn[224] in the extracellular region (Figure 1). In general, N-glycosylation of proteins can play an important role in a variety of aspects, such as ligand binding, protein folding, trafficking, and stability.[14−16,33,34] We have previously found that enzymatic deglycosylation of IL5Rα weakened its ability to bind IL5.[13] However, it has remained unclear whether all of the N-glycosylations are involved in ligand binding or if only a specific subset of N-glycosylation sites is necessary. It also was unclear what caused such a drastic loss of ligand binding. To answer these questions, we investigated the structural and functional roles of N-glycosylation sites by site-directed mutagenesis. We initially introduced an Asn-to-Gln mutation as one of the general approaches to mutational deglycosylation. However, we found that such a mutation caused significant decreases in the level of protein expression (data not shown) as well as losses of binding to its conformationally sensitive antibody (Figure 3), suggesting that introduction of glutamine at these points destabilizes the structure of IL5Rα. Therefore, we evaluated the ability of a series of combinatorial and rationally designed mutations to preserve the stability of deglycosylated mutants of IL5Rα. The former approach is based on a hypothesis that asparagine residues at the N-glycosylation sites can be replaced with certain charged residues while maintaining the stability of the protein.[18] The latter approach is based on a finding that the
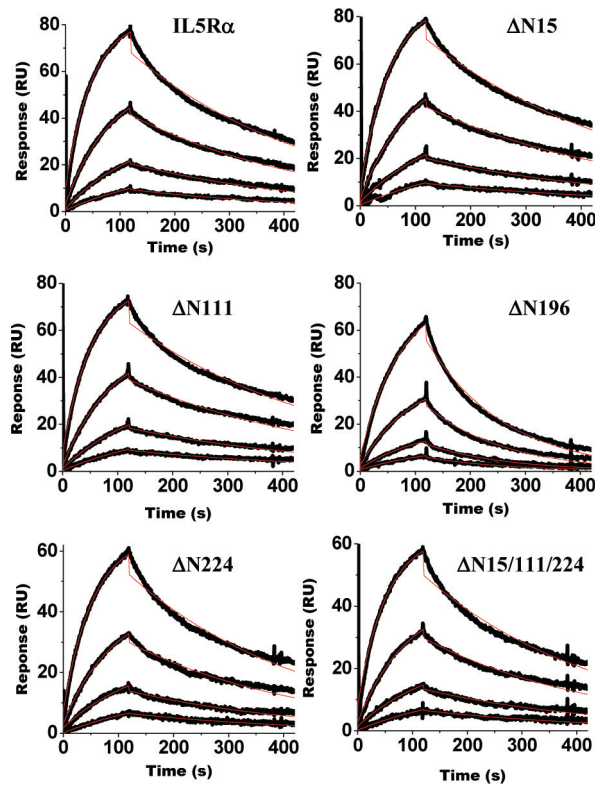
Figure 4. Ligand binding of deglycosylated variants. The soluble forms of wild-type IL5Rα and five deglycosylation mutants were transiently expressed in S2 cells, and the supernatants were injected over the anti-V5-tag antibody biosensor chip surface on the biosensor ("on-chip purification"). Subsequently, various concentrations (5, 10, 20, and 40 nM) of IL5 were injected at 0 s, followed by injection of running buffer alone at 120 s. The rate constants were calculated by globally fitting the association phase (0−120 s) and the dissociation phase (120−360 s) to a model for 1:1 Langmuir binding. Red lines show calculated sensorgrams. Individual kinetic parameters were obtained from three separate experiments. The average and standard deviation are listed in Table 1.

stability and solubility of glycan-free forms of glycoproteins can be improved by using apolar-to-polar mutations of any surface residue in functionally irrelevant epitopes.[17] We utilized a conformationally sensitive anti-IL5Rα mAb as a marker to verify the structural integrity of IL5Rα and performed a medium-throughput assay of all the deglycosylated mutants with a surface plasmon resonance (SPR) biosensor (Figure 2).

From these two protein engineering approaches, we generated a total of 54 deglycosylation mutations (Figure 3). We found that mutations such as N15D, N111D, and N224R displayed significantly increased structural stability relative to the Asn-to-Gln mutation, while any replacement at Asn[196]

Table 2. Comparison of Carbohydrate Contents of Wild-Type and Mostly Deglycosylated IL5Rα Determined by MALDI-TOF MS

	MS(calc)	MS(exp)	ΔMS(exp−calc)	ΔMS(wt mutant)
IL5Rα	35877	41750	5873	−
IL5Rα[ΔN15/111/224]	36447	38791	2344	3529

severely reduced stability (Figure 3A,B). Interestingly, Asn-to-Asp mutations were more stable than Asn-to-Glu or Asn-to-Gln mutations at Asn[15], Asn[111], and Asn[224], suggesting that not only the charge of an amino acid but also its molecular volume might be important for the stability of local structure. These data imply that the Asn-to-Gln mutation, which is generally chosen for deglycosylation because of the retention of electrostatic properties, may not be the best strategy for all glycoproteins. Although any replacement at Asn[196] with charged residues severely reduced stability, substitution with threonine gave the best result (Figure 3B). It should be noted that threonine is the residue at the corresponding position of the human prolactin receptor in our sequence alignment (Figure 1). From rationally designed mutations, we found that IL5Rα[ΔN111] (I109V/V110T/N111D) and IL5Rα[ΔN224] (L223R/N224Q) had almost the same structural stability as the fully glycosylated form of IL5Rα (Figure 3C).

Because IL5Rα[ΔN15], IL5Rα[ΔN111], and IL5Rα-[ΔN224] mutants have almost the same stability and binding affinity for IL5 (Figure 4 and Table 1), we engineered a deglycosylated variant from which three of four glycosylation sites have been eliminated. This mostly deglycosylated variant (denoted IL5Rα[ΔN15/111/224]) also exhibited the same binding affinity for IL5 as fully glycosylated IL5Rα. We sought a rationale for these stability-preserving mutations in a homology-modeled structure of IL5Rα[ΔN15/111/224]. We found that mutations such as N15D and L223R/N224Q might stabilize the structure through interactions with neighboring charged residues. In the model, the side chain of Asp[15] appears to interact with the side chain of Lys[19] (Figure 6A), and therefore, the Asn-to-Gln mutation at this position would be expected to lead to a loss of a favorable charge interaction. The side chains of Arg[223] and Gln[224] appear to stabilize the interstrand conformation by interacting with the side chain of Glu[239] in the neighboring strand (Figure 6B). In contrast, no favorable interactions of mutated residues in the N111 region (I109V/V110T/N111Q) were observed with neighboring residues in the modeled structure, even though the I109V/V110T/N111Q mutant preserved the stability to the same extent as fully glycosylated IL5Rα. Perhaps the combination of apolar and polar groups in this locus is sufficient to contribute entropically to the stabilization of the protein. One could imagine that Asn-to-Gln mutation alone at positions 111 and

Table 1. Kinetic Interaction between IL5 and Soluble Forms of IL5Rα Deglycosylated Variants

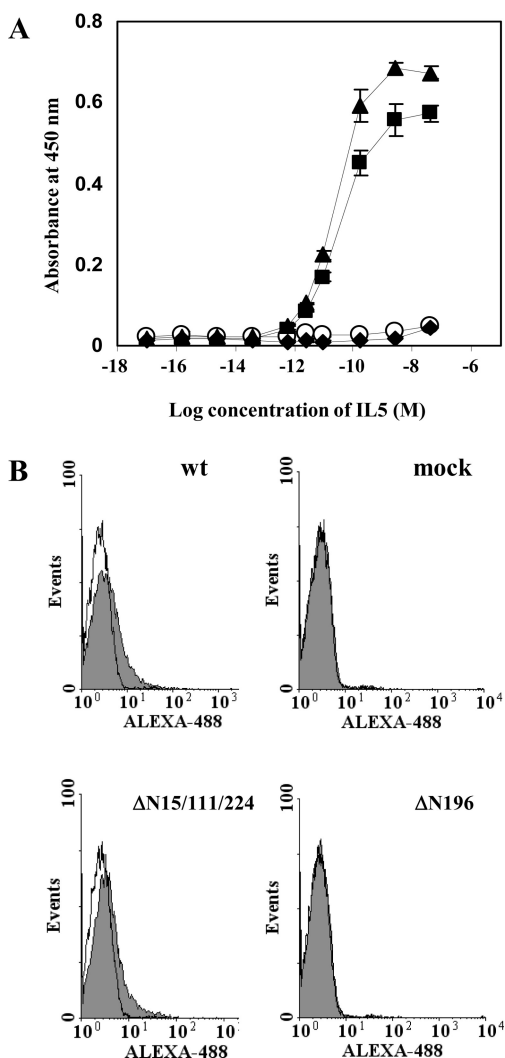|	mutations	k_{on} (×10^{-6} M^{-1} s^{-1})	k_{off} (×10^{3} s^{-1})	K_d (×10^{9} M)
wild-type IL5Rα		1.2 ± 0.3	3.1 ± 0.1	2.7 ± 0.1
IL5Rα[ΔN15]	N15D	1.0 ± 0.8	2.5 ± 0.1	2.5 ± 0.2
IL5Rα[ΔN111]	I109V/V110T/N111D	1.1 ± 0.7	3.0 ± 0.2	2.7 ± 0.1
IL5Rα[ΔN196]	N196T	0.47 ± 0.3	7.1 ± 0.1	15 ± 1
IL5Rα[ΔN224]	L223R/N224Q	1.0 ± 0.4	3.3 ± 0.2	3.3 ± 0.1
IL5Rα[ΔN15/111/224]	N15D, I109V/V110T/N111D, and L223R/N224Q	1.0 ± 0.3	3.4 ± 0.2	3.2 ± 0.2

Figure 5. Cell proliferation activity and cell surface expression of full-length IL5Rα deglycosylation mutants. (A) The IL3-dependent mouse BaF3 cell line was used to test the bioactivity of exogenously expressed full-length IL5Rα (▲), full-length IL5Rα[ΔN15/111/224] (■), full-length IL5Rα[ΔN196] (♦), and empty vector (○). Five thousand cells per well were incubated with various dilutions (0.01 fM to 40 nM) of IL5. After incubation for 48 h, proliferation was evaluated as described in Experimental Procedures. The average values of triplicate wells are plotted with standard deviations. (B) Cytofluorometric analysis of cellular surface expression of the wild type and mutant of full-length IL5Rα on BaF3 transfectants. Cells were incubated with anti-IL5Rα antibodies or negative control (17b) as the primary antibody and Alexa-conjugated goat anti-mouse pAb (Invitrogen) as the secondary antibody. Histogram plots from 2B6R (gray area) show the expression of full-length forms of wild-type IL5Rα (wt) and IL5Rα[ΔN15/111/224] (ΔN15/111/224) compared to no expression of empty vector (mock) and IL5Rα[ΔN196] (ΔN196). The negative control indicates staining with the secondary antibody alone (black lines).

Figure 6. Potential charged interactions and hydrogen bonds introduced by the mutations at N-glycosylation sites. The homology-modeled structure of IL5Rα[ΔN15/111/224], based on a previously reported model of IL5Rα, suggests potential favorable interactions upon deglycosylation mutation at Asn[15] (A) and Asn[224] (B). The residues of interest are shown as a CPK model. Oxygen and nitrogen atoms are colored red and blue, respectively. All the molecular graphics in this article were prepared with RasMol.[50]

IL5Rα is a member of the class I cytokine receptor superfamily, members of which are characterized by the presence of the so-called cytokine recognition motif.[35] Extensive structural studies have been performed for various cytokine−receptor complexes in this superfamily (reviewed in references 36 and 37). In some cases (e.g., G-CSF[38]), crystal structures of the cytokine−receptor complex have been determined without deglycosylation. However, early trials to obtain crystals of the fully glycosylated IL5Rα in complex with deglycosylated IL5 proved unsuccessful.[13] Because carbohydrate moieties of glycoproteins affect crystal formation, deglycosylation prior to crystallization could improve the chances for obtaining high-quality crystals. For deglycosylation of the cytokine receptors, the following four methods have been used: bacterial expression (e.g., growth hormone,[29] prolactin,[30] and IL4[39]), enzymatic deglycosylation (e.g., IL10[40] and IL12[41]), mutational deglycosylation (e.g., erythropoietin[42] and IL6[43]), and inhibition of glycosidase (e.g., IL2[44]). Most recently, Hansen et al. have successfully determined the crystal structure of the receptor complex of GM-CSF, which is the closest homologue of IL5, by using GM-CSF from bacterial expression, a fully glycosylated α subunit, and a βc subunit with Asn-to-Gln mutational deglycosylation.[45] Here, we utilized site-directed mutagenesis and engineered IL5Rα[ΔN15/111/224], which retained Asn[196], while eliminating the other three glycosylation sites of IL5Rα. This mostly deglycosylated variant might facilitate crystallization of the IL5−receptor complex, and the stability-preserving deglycosylation strategies presented here could be applied to crystallographic analyses of other glycoproteins.

Our data demonstrated that deglycosylation at Asn[196] of IL5Rα severely reduced its stability and binding affinity for IL5

224 might not be sufficient to stabilize the local conformation without other favorable interactions or increased hydrophilicity at nearby mutational sites. In any case, the model suggests that some carbohydrate moieties of IL5Rα could be replaced without compromising the stability and function of IL5Rα protein.
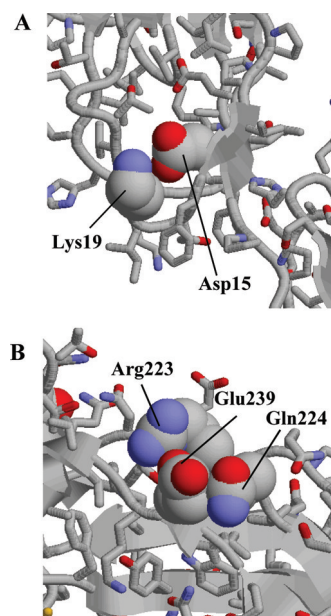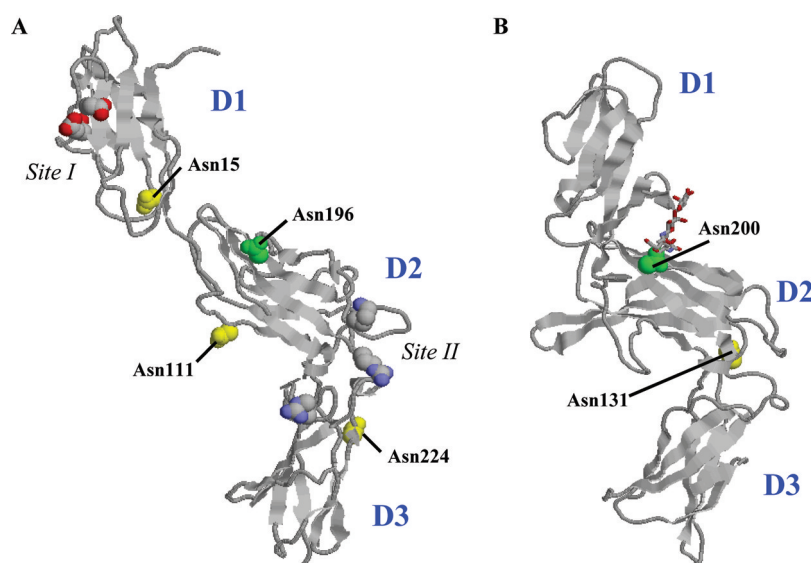
Figure 7. Maps of the N-glycosylation sites and ligand binding epitopes on the homology-modeled structure of IL5Rα compared with the crystal structure of IL12. (A) Modeled structure of IL5Rα.[12] (B) Crystal structure of IL12 p40.[41] Three fibronectin type III domains (D1, D2, and D3) are denoted from the N- to C-terminus. Asn[196] of IL5Rα and Asn[200] of IL12 are colored green, and other asparagine residues for N-glycosylation are colored yellow. The IL5-binding residues at site I and II epitopes, which have been found previously,[12,32] are shown as a CPK model. The loop regions are represented as coils and β strands as ribbons. Carbohydrate groups are shown as stick models. GlcNAc and Man stand for *N*-acetylglucosamine and mannose, respectively.

(Figure 3 and Figure 4). We also observed that IL5Rα[ΔN196] lost ligand binding activity over time (data not shown). These findings inspired us to test whether deglycosylation at Asn[196] of IL5Rα caused a reduction in the ligand binding activity not because the carbohydrate is involved in the direct interaction with the ligand but as a secondary effect of the partially destabilized structure of IL5Rα upon deglycosylation. We have previously shown that IL5-binding residues are located in the D1 domain (Asp[55], Asp[56], and Glu[58]) as well as in the D2 domain (Lys[186] and Arg[188]) and the D3 domain (Arg[297]).[12] The binding interface of IL5Rα comprises a cluster of negatively charged residues [site I epitope (Figure 7A)] from the D1 domain and a cluster of positively charged residues [site II epitope (Figure 7A)] from the D2D3 tandem domain. The homology-deduced IL5Rα structure shows that Asn[196] in the D2 domain is not located in the proximity of either site I or II epitopes (Figure 7A). The four N-glycosylation sites of IL5Rα are conserved in GM-CSF receptor α, which shares a high degree of amino acid sequence similarity with IL5Rα as well as signaling receptor βc (sequence alignment available in reference 32). The crystal structure of the GM-CSF receptor complex showed no direct interaction of the receptor carbohydrate and ligand.[45] Moreover, our lectin inhibition assay showed that neither cyanovirin-N nor concanavalin-A had any impact on the interaction of IL5Rα[ΔN15/111/224] with deglycosylated IL5 (Figure S2 of the Supporting Information). From these observations, we conclude that the carbohydrate at Asn[196] is less likely involved in the direct interaction between IL5 and IL5Rα and instead likely plays a critical role in maintaining the correct structure of the receptor. Interestingly, Yoon et al.[41] found that a carbohydrate extending from Asn[200] of the D2 domain lies in the interface of the D1 and D2 domains in the crystal structure of the p35–p40 heterodimer of IL12 (Figure 7B). They have proposed that the carbohydrate stabilizes the structure by fixing the relative orientation of these domains through hydrogen bonds and van der Waals contacts. It is

noteworthy that the spatial position of Asn[196] of IL5Rα is similar to that of Asn[200] of IL12 (Figure 7). Although the detailed structural role of the carbohydrate at Asn[196] of IL5Rα must await high-resolution structure determination of the IL5–IL5Rα[ΔN15/111/224] complex by X-ray crystallography, it is tempting to speculate that the carbohydrate at Asn[196] might stabilize the overall structure of the receptor by bridging the D1 and D2 domains as in the IL12 system.

We developed a medium-throughput screening assay to characterize the structural integrity and ligand binding affinity of the extracellular domain of IL5Rα by using the transient expression system with *Drosophila* S2 insect cells. Although insect expression facilitates overexpression and screening of a large number of recombinant proteins, it is known that the carbohydrate components of N-glycosylation of insect cells are different from those of mammalian cells.[46,47] To verify the role of N-glycosylation of IL5Rα in mammalian cells, we used the BaF3 cell line, a mouse pro B cell line that has been used for functional analyses of human IL5Rα.[25,48] Using BaF3 cells expressing full-length IL5Rα and its mutational variants, we found that deglycosylation at Asn[196] resulted in the failure of cell surface expression of IL5Rα (Figure 5B) and caused a complete loss of the biological response to IL5 (Figure 5A). In light of the finding that the carbohydrate at Asn[196] is likely indispensable for the correct structure of the receptor (see above), it is plausible that Asn[196] deglycosylation causes the failure of cell surface expression of IL5Rα[ΔN196] by destabilizing the structure of IL5Rα.

In conclusion, this study reveals the essential role of a single carbohydrate moiety at Asn[196] in the structure and function of IL5Rα. Our unique protein engineering approach also demonstrated that most, but not all, N-linked carbohydrates can be eliminated without compromising the function of the protein via introduction of targeted mutations at and around N-glycosylation sites. We obtained a stable and functional variant that has three of four glycosylation sites eliminated. The mostly

deglycosylated form we obtained in this study could open the way to improving high-resolution structural analysis of the IL5 system and help in the design of new compounds for therapeutic treatment of IL5-related allergic inflammatory diseases.

■ ASSOCIATED CONTENT

⑤ Supporting Information

Biosensor data of kinetic interaction of lectin and IL5Rα deglycosylation variants. This material is available free of charge via the Internet at http://pubs.acs.org.

■ AUTHOR INFORMATION

Corresponding Author
*E-mail: Irwin.Chaiken@DrexelMed.edu. Phone: (215) 762-4197. Fax: (215) 762-4452.

Present Address
[⊥]Pfizer Global Research & Development, 87 Cambridgepark Dr., Cambridge, MA 02140.

■ ACKNOWLEDGMENTS

We thank Dr. Keith A. Vosseller (Drexel University College of Medicine) for the useful discussion.

■ ABBREVIATIONS

IL5Rα, human interleukin-5 receptor α; GM-CSF, granulocyte/macrophage colony-stimulating factor; PBS, phosphate-buffered saline; SPR, surface plasmon resonance; RU, resonance unit; GFP, green fluorescent protein; ConA, concanavalin A; CV-N, cyanovirin-N; mAb, monoclonal antibody; pAb, polyclonal antibody; ΔN15, N15D mutant of IL5Rα; ΔN111, I109V/V110T/N111D mutant of IL5Rα; ΔN196, N196T mutant of IL5Rα; ΔN224, L223R/N224Q mutant of IL5Rα; ΔN15/111/224, N15/I109V/V110T/N111D/L223R/N224Q mutant of IL5Rα.

■ REFERENCES

(1) Karlen, S., De Boer, M. L., Lipscombe, R. J., Lutz, W., Mordvinov, V. A., and Sanderson, C. J. (1998) Biological and molecular characteristics of interleukin-5 and its receptor. *Int. Rev. Immunol. 16*, 227–247.

(2) Sanderson, C. J., and Urwin, D. (2000) Interleukin-5: A drug target for allergic diseases. *Curr. Opin. Invest. Drugs 1*, 435–441.

(3) Foster, P. S., Hogan, S. P., Yang, M., Mattes, J., Young, I. G., Matthaei, K. I., Kumar, R. K., Mahalingam, S., and Webb, D. C. (2002) Interleukin-5 and eosinophils as therapeutic targets for asthma. *Trends Mol. Med. 8*, 162–167.

(4) Rothenberg, M. E. (2004) Eosinophilic gastrointestinal disorders (EGID). *J. Allergy Clin. Immunol. 113*, 11–28.

(5) Zaks-Zilberman, M., Harrington, A. E., Ishino, T., and Chaiken, I. M. (2008) Interleukin-5 receptor subunit oligomerization and rearrangement revealed by fluorescence resonance energy transfer imaging. *J. Biol. Chem. 283*, 13398–13406.

(6) Ishino, T., Harrington, A. E., Zaks-Zilberman, M., Scibek, J. J., and Chaiken, I. (2008) Slow-dissociation effect of common signaling subunit βc on IL5 and GM-CSF receptor assembly. *Cytokine 42*, 179–190.

(7) Scibek, J. J., Evergren, E., Zahn, S., Canziani, G. A., Van Ryk, D., and Chaiken, I. M. (2002) Biosensor analysis of dynamics of interleukin 5 receptor subunit βc interaction with IL5:IL5Rα complexes. *Anal. Biochem. 307*, 258–265.

(8) Carr, P. D., Gustin, S. E., Church, A. P., Murphy, J. M., Ford, S. C., Mann, D. A., Woltring, D. M., Walker, I., Ollis, D. L., and Young, I. G. (2001) Structure of the complete extracellular domain of the common β subunit of the human GM-CSF, IL-3, and IL-5 receptors reveals a novel dimer configuration. *Cell 104*, 291–300.

(9) Morton, T., Li, J., Cook, R., and Chaiken, I. (1995) Mutagenesis in the C-terminal region of human interleukin 5 reveals a central patch for receptor α chain recognition. *Proc. Natl. Acad. Sci. U.S.A. 92*, 10879–10883.

(10) Tavernier, J., Tuypens, T., Verhee, A., Plaetinck, G., Devos, R., Van der Heyden, J., Guisez, Y., and Oefner, C. (1995) Identification of receptor-binding domains on human interleukin 5 and design of an interleukin 5-derived receptor antagonist. *Proc. Natl. Acad. Sci. U.S.A. 92*, 5194–5198.

(11) Cornelis, S., Plaetinck, G., Devos, R., Van der Heyden, J., Tavernier, J., Sanderson, C. J., Guisez, Y., and Fiers, W. (1995) Detailed analysis of the IL-5-IL-5Rα interaction: Characterization of crucial residues on the ligand and the receptor. *EMBO J. 14*, 3395–3402.

(12) Ishino, T., Pasut, G., Scibek, J., and Chaiken, I. (2004) Kinetic interaction analysis of human interleukin 5 receptor α mutants reveals a unique binding topology and charge distribution for cytokine recognition. *J. Biol. Chem. 279*, 9547–9556.

(13) Johanson, K., Appelbaum, E., Doyle, M., Hensley, P., Zhao, B., Abdel-Meguid, S. S., Young, P., Cook, R., Carr, S., Matico, R., et al. (1995) Binding interactions of human interleukin 5 with its receptor α subunit. Large scale production, structural, and functional studies of *Drosophila*-expressed recombinant proteins. *J. Biol. Chem. 270*, 9459–9471.

(14) West, C. M. (1986) Current ideas on the significance of protein glycosylation. *Mol. Cell. Biochem. 72*, 3–20.

(15) Helenius, A. (1994) How N-linked oligosaccharides affect glycoprotein folding in the endoplasmic reticulum. *Mol. Biol. Cell 5*, 253–265.

(16) Niu, L., Heaney, M. L., Vera, J. C., and Golde, D. W. (2000) High-affinity binding to the GM-CSF receptor requires intact N-glycosylation sites in the extracellular domain of the β subunit. *Blood 95*, 3357–3362.

(17) Sun, Z. Y., Dotsch, V., Kim, M., Li, J., Reinherz, E. L., and Wagner, G. (1999) Functional glycan-free adhesion domain of human cell surface receptor CD58: Design, production and NMR studies. *EMBO J. 18*, 2941–2949.

(18) Narhi, L. O., Arakawa, T., Aoki, K., Wen, J., Elliott, S., Boone, T., and Cheetham, J. (2001) Asn to Lys mutations at three sites which are N-glycosylated in the mammalian protein decrease the aggregation of *Escherichia coli*-derived erythropoietin. *Protein Eng. 14*, 135–140.

(19) Wu, S. J., Tambyraja, R., Zhang, W., Zahn, S., Godillot, A. P., and Chaiken, I. (2000) Epitope randomization redefines the functional role of glutamic acid 110 in interleukin-5 receptor activation. *J. Biol. Chem. 275*, 7351–7358.

(20) McFadden, K., Cocklin, S., Gopi, H., Baxter, S., Ajith, S., Mahmood, N., Shattock, R., and Chaiken, I. (2007) A recombinant allosteric lectin antagonist of HIV-1 envelope gp120 interactions. *Proteins 67*, 617–629.

(21) Tavernier, J., Van der Heyden, J., Verhee, A., Brusselle, G., Van Ostade, X., Vandekerckhove, J., North, J., Rankin, S. M., Kay, A. B., and Robinson, D. S. (2000) Interleukin 5 regulates the isoform expression of its own receptor α-subunit. *Blood 95*, 1600–1607.

(22) Pace, C. N., Vajdos, F., Fee, L., Grimsley, G., and Gray, T. (1995) How to measure and predict the molar absorption coefficient of a protein. *Protein Sci. 4*, 2411–2423.

(23) Dowd, C. S., Leavitt, S., Babcock, G., Godillot, A. P., Van Ryk, D., Canziani, G. A., Sodroski, J., Freire, E., and Chaiken, I. M. (2002) β-turn Phe in HIV-1 Env binding site of CD4 and CD4 mimetic

miniprotein enhances Env binding affinity but is not required for activation of co-receptor/17b site. *Biochemistry 41*, 7038−7046.

(24) Myszka, D. G. (2000) Kinetic, equilibrium, and thermodynamic analysis of macromolecular interactions with BIACORE. *Methods Enzymol. 323*, 325−340.

(25) Cornelis, S., Fache, I., Van derHeyden, J., Guisez, Y., Tavernier, J., Devos, R., Fiers, W., and Plaetinck, G. (1995) Characterization of critical residues in the cytoplasmic domain of the human interleukin-5 receptor α chain required for growth signal transduction. *Eur. J. Immunol. 25*, 1857−1864.

(26) Sali, A., and Blundell, T. L. (1993) Comparative protein modelling by satisfaction of spatial restraints. *J. Mol. Biol. 234*, 779−815.

(27) Laskowski, R., MacArthur, M., Moss, D., and Thornton, J. (1993) PROCHECK: A program to check the stereochemical quality of protein structures. *J. Appl. Crystallogr. 26*, 283−291.

(28) Sippl, M. J. (1993) Recognition of errors in three-dimensional structures of proteins. *Proteins 17*, 355−362.

(29) de Vos, A. M., Ultsch, M., and Kossiakoff, A. A. (1992) Human growth hormone and extracellular domain of its receptor: Crystal structure of the complex. *Science 255*, 306−312.

(30) Somers, W., Ultsch, M., De Vos, A. M., and Kossiakoff, A. A. (1994) The X-ray structure of a growth hormone-prolactin receptor complex. *Nature 372*, 478−481.

(31) Ishino, T., Pillalamarri, U., Panarello, D., Bhattacharya, M., Urbina, C., Horvat, S., Sarkhel, S., Jameson, B., and Chaiken, I. (2006) Asymmetric usage of antagonist charged residues drives interleukin-5 receptor recruitment but is insufficient for receptor activation. *Biochemistry 45*, 1106−1115.

(32) Ishino, T., Urbina, C., Bhattacharya, M., Panarello, D., and Chaiken, I. (2005) Receptor epitope usage by interleukin 5 mimetic peptide. *J. Biol. Chem. 280*, 22951−22961.

(33) Waetzig, G. H., Chalaris, A., Rosenstiel, P., Suthaus, J., Holland, C., Karl, N., Valles Uriarte, L., Till, A., Scheller, J., Grotzinger, J., Schreiber, S., Rose-John, S., and Seegert, D. (2010) N-linked glycosylation is essential for the stability but not the signaling function of the interleukin-6 signal transducer glycoprotein 130. *J. Biol. Chem. 285*, 1781−1789.

(34) McElroy, C. A., Dohm, J. A., and Walsh, S. T. (2009) Structural and biophysical studies of the human IL-7/IL-7Rα complex. *Structure 17*, 54−65.

(35) Taniguchi, T. (1995) Cytokine signaling through nonreceptor protein tyrosine kinases. *Science 268*, 251−255.

(36) Walter, M.R. (2002) Crystal structures of α-helical cytokine-receptor complexes: We've only scratched the surface. *Biotechniques 46−48* (Suppl.), 50−47.

(37) Wang, X., Lupardus, P., Laporte, S. L., and Garcia, K. C. (2009) Structural Biology of Shared Cytokine Receptors. *Annu. Rev. Immunol. 27*, 29−60.

(38) Aritomi, M., Kunishima, N., Okamoto, T., Kuroki, R., Ota, Y., and Morikawa, K. (1999) Atomic structure of the GCSF-receptor complex showing a new cytokine-receptor recognition scheme. *Nature 401*, 713−717.

(39) Hage, T., Sebald, W., and Reinemer, P. (1999) Crystal structure of the interleukin-4/receptor α chain complex reveals a mosaic binding interface. *Cell 97*, 271−281.

(40) Josephson, K., Logsdon, N. J., and Walter, M. R. (2001) Crystal structure of the IL-10/IL-10R1 complex reveals a shared receptor binding site. *Immunity 15*, 35−46.

(41) Yoon, C., Johnston, S. C., Tang, J., Stahl, M., Tobin, J. F., and Somers, W. S. (2000) Charged residues dominate a unique interlocking topography in the heterodimeric cytokine interleukin-12. *EMBO J. 19*, 3530−3541.

(42) Syed, R. S., Reid, S. W., Li, C., Cheetham, J. C., Aoki, K. H., Liu, B., Zhan, H., Osslund, T. D., Chirino, A. J., Zhang, J., Finer-Moore, J.,

Elliott, S., Sitney, K., Katz, B. A., Matthews, D. J., Wendoloski, J. J., Egrie, J., and Stroud, R. M. (1998) Efficiency of signalling through cytokine receptors depends critically on receptor orientation. *Nature 395*, 511−516.

(43) Boulanger, M. J., Chow, D. C., Brevnova, E. E., and Garcia, K. C. (2003) Hexameric structure and assembly of the interleukin-6/IL-6 α-receptor/gp130 complex. *Science 300*, 2101−2104.

(44) Wang, X., Rickert, M., and Garcia, K. C. (2005) Structure of the quaternary complex of interleukin-2 with its α, β, and γ receptors. *Science 310*, 1159−1163.

(45) Hansen, G., Hercus, T. R., McClure, B. J., Stomski, F. C., Dottore, M., Powell, J., Ramshaw, H., Woodcock, J. M., Xu, Y., Guthridge, M., McKinstry, W. J., Lopez, A. F., and Parker, M. W. (2008) The structure of the GM-CSF receptor complex reveals a distinct mode of cytokine receptor activation. *Cell 134*, 496−507.

(46) Davidson, D. J., and Castellino, F. J. (1991) Structures of the asparagine-289-linked oligosaccharides assembled on recombinant human plasminogen expressed in a *Mamestra brassicae* cell line (IZD-MBO503). *Biochemistry 30*, 6689−6696.

(47) Benting, J., Lecat, S., Zacchetti, D., and Simons, K. (2000) Protein expression in *Drosophila* Schneider cells. *Anal. Biochem. 278*, 59−68.

(48) Czabotar, P. E., Holland, J., and Sanderson, C. J. (2000) Identification of regions within the third FnIII-like domain of the IL-5Rα involved in IL-5 interaction. *Cytokine 12*, 867−873.

(49) Thompson, J. D., Higgins, D. G., and Gibson, T. J. (1994) CLUSTAL W: Improving the sensitivity of progressive multiple sequence alignment through sequence weighting, position-specific gap penalties and weight matrix choice. *Nucleic Acids Res. 22*, 4673−4680.

(50) Sayle, R. A., and Milner-White, E. J. (1995) RASMOL: Biomolecular graphics for all. *Trends Biochem. Sci. 20*, 374.